DELFT UNIVERSITY OF TECHNOLOGY

Automating AC Power Flow Simulations

The European Electricity Grid

Interim Thesis Report

Author:
Shravan Chipli

Supervisors TU Delft:
Prof.dr.ir. C. Vuik
M.E. Kootte

Supervisors TenneT:
Martin Wevers
Jorrit Bos

February 2021

Foreword

This MSc graduation project is being done in the group of Numerical Mathematics, TU Delft, in collaboration with TenneT TSO B.V. TenneT is a European electricity transmission system operator (TSO) that manages the high-voltage grid in the Netherlands and large parts of Germany.

The power flow problem or the load flow problem involves determining the voltage magnitudes and phase angles in every bus of the power system. These quantities are then used to compute the power flow in every branch of the power system network. This constitutes the steady state power flow simulations which, for given generation and consumption, give insight into the steady state behavior of the network. Hence, power flow simulations play a fundamental role in various sectors of a TSO such as operation and planning.

In this interim thesis report, we present the findings of a literature study conducted in order to understand the theory behind solving the power flow problem and to hence achieve the research objectives of this project.

Contents

Chapter 1

Introduction

The goal of this project is to develop an AC power flow solver for the European electricity transmission network that includes the Netherlands, Germany, Belgium, Luxembourg and France (fig. 1.1 shows TenneT's high voltage grid), and automate calculations in order to speed up tasks such as voltage regulation and reactive power compensation assessments for transmission system planning. In the context of year-round calculations, a comparison between AC and DC approaches of solving the power flow problem will be made.

Motivation

A TSO is responsible for safe and reliable transport of electric power. One of the key challenges to ensure safety and reliability is to keep the voltages within safe limits across the transmission network. The rapid increase in addition of Renewable Energy Sources (RES) into electricity networks causes voltage fluctuations to occur more frequently. For instance, excess wind and solar generation would cause the voltages in the transmission network to increase beyond the safe operating limit. To manage such situations best in the future, clever planning of the essential infrastructure is necessary.

It is best practice for a TSO to keep the voltages within limits just by using reactive power compensating assets such as shunt reactors and capacitor banks in normal operating conditions. However, extreme operating conditions call for additional reactive power support from generators, which is expensive and generally not desired. It seems quite rational to anticipate abnormal operating conditions considering the stochastic nature of growing renewable energy sources and extreme weather conditions. Hence, it is very important for a TSO to efficiently plan for reactive power compensating assets for the decades to come.

AC year-round simulations help to estimate the need for reactive power compensating assets. TenneT currently uses commercial software packages for power flow analysis. With increasing problem sizes and widely varying inputs, it has been found that the grid models often run into convergence issues when solving the AC power flow problem. This means that the power flow problem could be ill-posed. Ensuring convergence and voltage regulation currently involve manual intervention. That is, manually adding external grids to achieve reactive power balance in the network or to change the voltage setpoints of generators. This is a trial and error technique that could fix the ill-posedness of the problem and get the model to converge. Once the model converges, voltages are kept within limits by manually switching shunt reactors or capacitor banks on/off. This is largely time consuming, especially for year-round simulations, wherein there could possibly be convergence issues in almost all hours of the year. Hence AC power flow simulations are currently done only for a few worst-case hours. In order to do AC year-round simulations, an automated solver that can fix convergence issues and regulate voltages without manual intervention is necessary. Moreover, the exact reason for the solvers to diverge is not yet known and most often, the tricks employed to get a grid model to converge do not work for a different model or for a different set of inputs.

In this project, we investigate convergence problems in detail and develop mathematical models that automatically ensure convergence and regulate voltages. The models could form the basis for a potential software subroutine that can perform AC year-round simulations for a wide range of inputs, without manual intervention.

Another important application of power flow simulations is capacity planning. As the name implies, capacity planning involves planning the transmission system infrastructure such as additional cables in the network for the future. Year-round power flow simulations are carried out in order to determine transmission line loading and thus plan the additional capacities required to operate the transmission system without overloading the lines in the network. TenneT currently uses the DC power flow approach to do year-round simulations for capacity planning. The DC approach is often favored for computational benefits and when AC power flow simulations cannot be done, for instance, due to convergence issues. However, since the DC approach linearizes the power flow problem, there could be a significant reduction in accuracy of the solution. For line loading, this means that the determined values could be less than that in reality, possibly leading to an inferior estimate of capacity requirements. In this project we quantify the reduction in accuracy by comparing the solution of the automated AC power flow simulation model with the DC solution. The advantages of using the AC power flow model for capacity planning, if any, will be weighed by a cost analysis.

Literature review

In order to solve the aforementioned problems, we start with a literature review that serves as a foundation to this project. The following four concepts of power flow analysis are studied.

- The power flow problem
- Power flow solvers

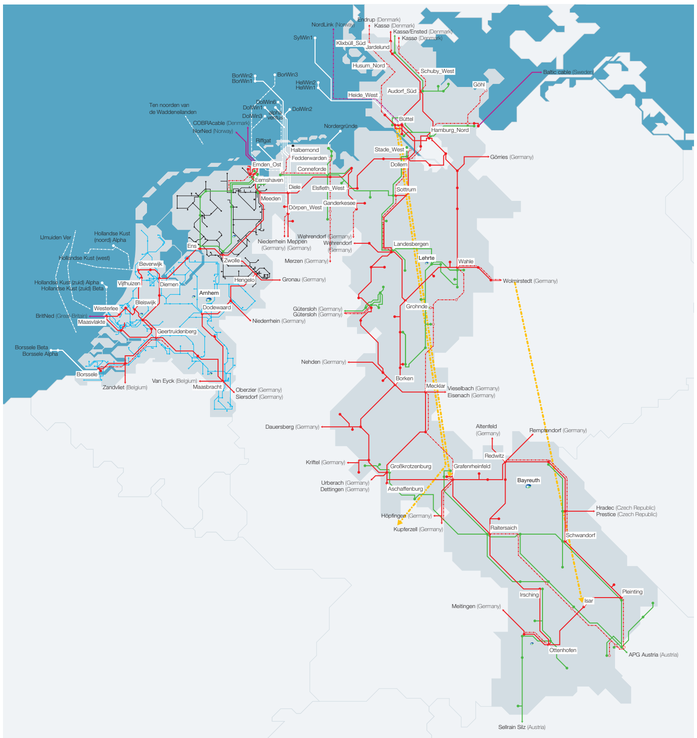

Figure 1.1: Grid map of TenneT

- Convergence properties of solvers
- Comparison of AC and DC approaches

The mathematical model of the transmission system is derived and studied in order to understand the power flow problem which lies at the heart of power flow analysis. To derive the mathematical model, we study the fundamentals of AC circuits and explore the transmission network topology. As solving the power flow problem requires a good understanding of the available power flow solvers, we investigate some of the prominent power flow solvers used in power flow analysis and understand their capabilities. The key to automate calculations is understanding the convergence properties of power flow solvers. We review some of the methods available in the literature that improve convergence of solvers. The feasibility of using the DC approximation method in place of a full power flow solver is investigated. A few software packages commonly used in the industry are introduced. The report starts with a brief introduction to electricity grids and concludes with the findings of the literature review and the research questions of the project.

Chapter 2

The Electric Grid

Electric grids are some of the largest networks humanity has ever built. For more than a hundred years[1] now, they have been doing an incredible job lighting up our societies. It's very hard to imagine life without electricity, for the world then would come to a halt.

The fact that electric power is just a switch away in most parts of the world today is a result of the intricate electric grids that quite seamlessly bridge generation and consumption. The complexity of electric grids is increasing at a rapid pace with integration of renewable energy sources. A strong mathematical approach and collective effort are imperative to understand, model, and control the electric grids of this day better.

This chapter briefly describes the fundamental stages of an electric grid and a few challenges down the road.

2.1 Generation

Conventionally, electric power is generated as Alternating Current (AC) at places known as power plants or generating stations. An *AC generator* transforms mechanical energy to electric energy by electromagnetic induction. The *prime movers* that drive generators could be steam/gas/water/wind turbines, internal combustion engines or nuclear reactors depending on location and availability of resources. For example, electricity in the Netherlands is produced primarily from natural gas and coal [2].

An exception to AC generation is the use of photovoltaic (PV) cells. PV cells transform solar energy to Direct Current (DC) which is then converted to AC by an *inverter* before injecting it into the grid. Solar farms are gaining ground in places with more sunlight across the world.

[1]World's first central electric generating station - The Pearl Street Station, began operation on 4 September 1882 [1].

Electric power is generated at a frequency of 50 or 60 Hz [3]. This has been widely accepted as the optimal frequency considering several applications on a wide scale over a long period of time. However, railways, airplanes, ships and oil rigs use different frequencies. Higher frequency systems have the advantage of a better power to weight ratio for machines [3].

2.2 Transmission and Distribution

The distinct advantage of alternating current is that it can be efficiently stepped up and down in voltage using a transformer [4]. High voltage power is preferred for transmission over large distances as resistive losses are less. The high voltage network called the *transmission system* is responsible for transporting electricity in the order of 110-380 kV from power plants to substations [5]. The rest of the grid constituting of medium and low voltage lines is called the *distribution system* and is responsible for distributing electric power to end users. The substations shift the voltage down to the order of 10-20 kV and finally distribution transformers that are locally installed step it further down to the order of utilization voltage ($<$1kV) making it suitable for domestic and commercial use. It should also be noted that high voltage DC (HVDC) is sometimes preferred to AC when transmission distances are long enough to justify a reduction in cost of conductors (three phase AC needs three cables whereas DC needs two) over AC/DC conversion costs.

Electric power is generated and transmitted in three phases for two significant reasons. One, it facilitates smooth conversion of energy by applying uniform torque on generators and motors, unlike single phase AC which results in pulsating torque. This is an engineering advantage as the rotors are well balanced. Two, it offers cost benefits as the same amount of power can be transmitted with fewer conductors when compared to single phase transmission. Currents and voltages add up to zero in a balanced three phase system, eliminating the need for a common return wire[2]. This is under the assumption that all loads have equal impedance[3]. However, in practice the impedances are slightly different, hence requiring a return wire to complete the circuit. This is achieved by connecting the combined return wires to the common ground[4] at both ends.

Transmission systems are modelled and analyzed as single phase AC systems for the very reason of being balanced. That is, currents and voltages are equal in magnitude in all three phases. Whereas in distribution systems, current and voltage magnitudes are different because of the difference in loads and hence distribution systems are modelled considering all three phases. In fact, it is interesting to note that residential and most commercial circuits run on single phase AC and have two wires, one live and the other neutral (return).

[2] The three return wires are combined as a single return wire.

[3] Impedance is the AC equivalent of resistance.

[4] In electric circuits, ground refers to an electrically neutral reference that has 0 voltage. In this context, it refers to the earth which acts as the return pathway of the circuit.

2.3 Consumption

Loads are devices that consume electric power and are characterized by impedance. Theoretically, they can be broadly classified as *resistive, inductive* and *capacitive* loads. Resistive loads are heating conductors that are seen in incandescent bulbs and heaters. Inductive loads are all kinds of motors, fluorescent lamps and the transformers used in power supplies. Capacitors generally do not do physical work like other loads but are part of electrical circuits [4]. Based on usage, loads can be classified as residential, commercial, industrial and electric railways. Another important category of loads is consumer electronics [4].

From the system and also modelling perspective, electric power consumption is considered as *aggregate* load that combines several consumers. This may include households, city blocks or entire cities and regions. Given that the electric power industry is largely customer driven, capacity planning and serving instantaneous demand are very crucial for grid operators. *Load forecasting* is a discipline in itself and plays an important role in uninterrupted supply of electricity. For an interesting read about energy markets, we refer to [6], section 3.6.

2.4 Challenges

The stochastic nature of renewable energy sources such as wind and sun poses unprecedented challenges to the electric grid. Solar and wind farms are highly uncertain in generating power and cause severe problems to grid stability, possibly resulting in overloading and blackouts. Decentralized power generation by small windmills and rooftop solar panels that are connected to the distribution system causes a change in power-flow direction. This results in two-way traffic, making grid control and even power-flow analysis a hard task. Electric vehicle charging is another difficult-to-predict scenario on the distribution side of the electric grid.

The largest power outage in history occurred in north-east India on 30, 31 July, 2012 and affected 620 million people. In 2016, a blackout occurred in South Australia due to storms that caused a cascading failure of the transmission system infrastructure, affecting 1.7 million people. In May 2020, TenneT declared emergency state due to a high voltage incident that occurred due to high RES infeed and low demands.

It is very likely that such events take place in the future owing to the rapid changes the electricity systems are experiencing lately.

Chapter 3

Modelling the Transmission System

Power flow analysis is the numerical analysis of the flow of electric power and involves determining the operating state of the entire power system. The *state* describes how the power system functions and helps to understand how the system responds to inputs. In this chapter we derive the mathematical model of the transmission system and define the power flow problem which is cardinal to power flow analysis.

3.1 Fundamentals of AC circuits

This section describes the characteristics of an AC circuit, as required to model the transmission system. Definitions and equations are based on *electric circuit theory*.

3.1.1 Current and Voltage

In an AC system, current and voltage are sinusoidal functions characterized by amplitude, frequency and phase. They are expressed as,

$$i(t) = I_{max} \sin(\omega t + \phi_I) \qquad v(t) = V_{max} \sin(\omega t + \phi_V) \tag{3.1}$$

where,

$$\begin{aligned} I_{max} &= \text{amplitude of current},\ A \\ V_{max} &= \text{amplitude of voltage},\ V \\ \omega &= \text{angular frequency},\ rad/s \\ t &= \text{time},\ s \\ \phi &= \text{phase shift},\ rad \end{aligned}$$

For load-flow calculations, average values of currents and voltages are preferred. Averaging is done by considering Root Mean Sqaure (RMS) values of current and voltage functions. Since sinusoidal functions are perfectly symmetric, the effective or rms value is $1/\sqrt{2}$ times the amplitude. Instantaneous current and voltage are now written as,

$$i(t) = \sqrt{2}|I| \sin(\omega t + \phi_I) \qquad v(t) = \sqrt{2}|V| \sin(\omega t + \phi_V) \tag{3.2}$$

where $|I|$ and $|V|$ are rms values which are calculated as follows.

$$|I| = \sqrt{\frac{1}{T}\int_0^T i^2(t)\,dt} \qquad |V| = \sqrt{\frac{1}{T}\int_0^T v^2(t)\,dt} \tag{3.3}$$

where $T = 2\pi/\omega$ [s] is the period of sine wave. Intuitively, rms value is equal to the DC equivalent that dissipates the same amount of electric power in a given resistor per unit time.

In balanced three phase systems, current and voltage are equal in magnitude in all three phases but shifted in phase by $2\pi/3$ rad. Consequently, the power flow problem is solved by considering only one phase and the other two phases are analyzed simply by incorporating the phase shift. Note that it is convention to use the cosine function to describe current and voltage in power flow analysis. For a balanced three phase system, the governing equations are,

$$i(t) = \sqrt{2}|I| \cos(\omega t - \phi - \delta) \qquad v(t) = \sqrt{2}|V| \cos(\omega t - \delta) \tag{3.4}$$

where $\delta = \{0, 2\pi/3, 4\pi/3\}$ rad is the phase shift between the three phases and ϕ is the phase shift between current and voltage.

3.1.2 Phasor notation

Steady-state power flow analysis can be considerably simplified by using *phasors* to represent sinusoidal current and voltage functions. A phasor is an arrow that is imagined to spin in the complex plane and it characterizes a sine wave by specifying its magnitude and angle. Length of the phasor corresponds to amplitude or rms value, its angle with respect to real axis corresponds to time and its rotation corresponds to angular frequency which is constant and is generally not considered for steady-state power flow calculations. Considering sinusoidal current and voltage expressions:

$$i(t) = I_{max} \cos(\omega t - \delta_I) \quad \text{and} \quad v(t) = V_{max} \cos(\omega t - \delta_V),$$

we use Euler's identity $e^{j\phi} = \cos\phi + j\sin\phi$ and obtain,

$$\begin{aligned} i(t) &= \sqrt{2}Re(|I|e^{j\delta_I}e^{j\omega t}) & v(t) &= \sqrt{2}Re(|V|e^{j\delta_V}e^{j\omega t}) \\ &= \sqrt{2}Re(Ie^{j\omega t}) & &= \sqrt{2}Re(Ve^{j\omega t}) \end{aligned} \tag{3.5}$$

where,

$$I = |I|e^{j\delta_I} \quad \text{and} \quad V = |V|e^{j\delta_V}$$

Here I and V are current and voltage phasors. In a balanced three phase system, current and voltage values of one phase can be used to determine values of other phases just by accordingly rotating the phasors.

3.1.3 Power

Considering the phase with $\delta = 0$ and equations (3.4), instantaneous power can be expressed as,

$$\begin{aligned} p(t) &= v(t)i(t) \\ &= \sqrt{2}|V|\cos(\omega t)\sqrt{2}|I|\cos(\omega t - \phi) \\ &= |V||I|\cos\phi[1 + \cos(2\omega t)] + |V||I|\sin\phi[\sin(2\omega t)] \\ &= P[1 + \cos(2\omega t)] + Q[\sin(2\omega t)] \end{aligned} \tag{3.6}$$

where $P = |V||I|\cos\phi$ is called active power and $Q = |V||I|\sin\phi$ is called reactive power.

As evident from equation (3.6), instantaneous power is made up of two sinusoidal components. The first component $P[1 + \cos(2\omega t)]$ is unidirectional with average value P and the second component $Q[\sin(2\omega t)]$ is bidirectional with an average of 0.

Active power P is measured in watts $[W]$. It represents the power actually transmitted or consumed by loads and is always positive. For instance, for purely resistive loads, active power corresponds entirely to conversion of electric energy to heat or light. Active power is also called real power or average power.

Reactive power Q is expressed in volt-ampere reactive $[Var]$. For loads with reactance, phase difference between current and voltage ϕ is not zero and it results in instantaneous power sometimes being negative which can be interpreted as power flowing backwards from the load to the generator. This power that is oscillated back and forth through the lines is exchanged between electric and magnetic fields and is not dissipated [4]. Reactive power is also called imaginary power.

Power factor, often abbreviated as p.f. is defined by $\cos\phi$. When current lags voltage, ϕ is positive and power factor is said to be lagging. When current leads voltage, ϕ is negative and power factor is said to be leading. As ϕ varies from 0 to $90°$, p.f. varies from 1 to 0 corresponding to the loads from being purely resistive to being purely inductive. A power factor of 1 is highly desired since lower power factors lead to increased currents and higher heating losses in the power system [3].

The vector sum of P and Q is called complex power and is expressed as,

$$\mathbf{S} = VI^* = P + jQ \tag{3.7}$$

where V and I are voltage and current phasors and I^* is the complex conjugate of I. Another important quantity is *apparent power* which is generally used to specify the rating of an electrical apparatus. It is the product of current and voltage, regardless of their phase shift. It is measured in volt-amperes [VA] and is written as,

$$S = |V||I| \tag{3.8}$$

3.1.4 Impedance and Admittance

In AC circuits, the opposition to flow of current is called impedance which is the vector sum of resistance and reactance. It is given by,

$$\mathbf{Z} = R + jX \tag{3.9}$$

where R is *resistance* (real part) and X is *reactance* (imaginary part). Impedance is measured in ohms [Ω] and comes with every device in an AC circuit. When X is positive, reactance is inductive and $jX = j\omega L$ where L is the inductance. When X is negative, reactance is capacitive and $jX = 1/j\omega C$ where C is the capacitance. Note that R, L and C are always positive. When X is zero, impedance is purely resistive, indicating that there are no inductors and capacitors in the circuit.

The inverse of impedance is called admittance denoted by **Y**. It is expressed as,

$$\mathbf{Y} = 1/\mathbf{Z} = G + jB \tag{3.10}$$

where G is called *conductance* and B, *susceptance*. Considering the magnitudes of G and B, admittance can be written as,

$$\mathbf{Y} = \frac{R}{Z^2} - j\frac{X}{Z^2} \tag{3.11}$$

where Z is the magnitude of **Z**. G,B and hence **Y** are measured in siemens [S].

Furthermore, Ohm's law is extended to AC circuits as follows.

$$V = ZI \text{ or } I = YV \tag{3.12}$$

3.1.5 Kirchhoff's Circuit Laws

Kirchhoff's Voltage Law (KVL) states that the sum of voltages around any closed loop in a circuit must be zero.

$$\sum_j V_j = 0 \tag{3.13}$$

where V_j is the voltage across component j in the closed loop.

Kirchhoff's Current Law (KCL) states that the currents entering and leaving any node in the circuit must add up to zero.

$$\sum_k I_{ik} = 0 \tag{3.14}$$

where I_{ik} is the current flowing from node i to node k.

Kirchhoff's laws are extensively used to calculate currents and voltages in electrical circuits.

3.1.6 Per unit system

It is common practice to normalize numerical values for ease of calculation. In *per unit* (pu) system, the quantities of interest are expressed in terms of *base value* as follows.

$$\text{per unit value} = \frac{\text{actual value}}{\text{base value}}$$

The per unit value is dimensionless. In power system analysis, voltages, currents, impedances and powers are normalized. One of the advantages of using pu system is that the numerical effect of an ideal transformer is reduced to that of a series impedance [7].

3.2 Network Topology

The transmission system is modelled as a network of nodes and edges. Nodes are called *buses* and they represent points in the circuit where system components such as loads, generators, tap transformers, phase shifters, shunts or substations are connected. Edges are transmission *lines* that connect buses and hence system components to each other. In this section, we look at the topology in detail and describe how the components are modelled.

3.2.1 Buses and lines

Buses are considered to be electrically distinct, meaning that there exists an impedance between them which sustains a potential difference. Each bus is characterized by the following four quantities.

- Voltage phasor magnitude, V
- Voltage phase angle, δ
- Injected active power, P
- Injected reactive power, Q

Furthermore, buses are distinguished based on the parameters specified or controlled by components that they are connected to. Following three types are commonly used in power flow analysis.

Load Bus: As loads signify power consumption, they are modelled as such. At each load bus, active power and reactive power are specified, which together constitute negative power injection. A load bus is called PQ bus, suggesting that P and Q are known. V and δ are unknown, corresponding to the fact that loads do not control voltage.

Generator Bus: Generators are known to have control over active power and voltage. Hence, a generator bus is referred to as PV bus. However, wind turbines do not have voltage control and they are treated as PQ buses with a positive P. Another exception is that some generators supply only active power and they are modelled as PQ buses with $Q = 0$. The following reason clarifies this approach.

As mentioned earlier, supply and demand in an electric grid should always be in balance. This is achieved by matching generation and consumption of active and reactive power. Generators are solely responsible for active power balance, whereas reactive power can also be balanced by using devices such as shunts[1]. Hence, generators are modelled as PV or PQ buses depending upon the parameters they control.

Slack Bus: The challenge with achieving power balance is that generation should also account for transmission losses which are not known in advance. For active power, the trick in practice is to make an empirical assumption of what the losses could be and get a fixed power dispatch from all generators except one[2]. This generator's output is said to be controllable. It takes up the slack by generating more power if losses are greater than expected or less power if losses are smaller. Likewise, in power flow analysis, the slack bus or swing bus is analogous to the variable generator. As real power balance is a manifestation of steady frequency and hence of voltage angle, the phase angle δ is specified in place of P for the slack bus. On the other hand, slack in reactive power is shared by shunts and all generators that dispatch reactive power. Hence, V is specified for the slack bus as it is equivalent to requiring a balanced reactive power[3]. Note that it is convention to use $\delta = 0$ for the slack bus. It acts as a global reference for timing.

Table 3.1 summarizes the above described distinction of buses and helps visualize the parameters. N is the total number of buses in the network and N_g is the number of generator buses.

Buses such as transmission substations that are not connected to generators or loads are modelled as loads with $P = Q = 0$. A bus can also have both generator and load connected. Such buses are modelled as PV buses with $P = P_{gen} + P_{load}$.

[1] Shunts are devices that inject or consume reactive power.

[2] Could also be a few but as done in literature, we consider them as one to substantiate a slack bus.

[3] For a more detailed description about buses and choice of variables, we refer to [4], section 7.2.

Table 3.1: Bus types and variables

Bus type	Number of buses	Known	Unknown
Slack bus	1	δ, $\|V\|$	P, Q
PV bus	N_g	P, $\|V\|$	δ, Q
PQ bus	$N - N_g - 1$	P, Q	δ, $\|V\|$

A transmission line is modelled as an impedance between two nodes i and j. The impedances of transmission lines are assumed to be time-invariant under any electric potential and current. This allows the application of Ohm's law to determine line currents. Since a balanced three phase system is modelled considering the single phase equivalent, all transmission lines in the model correspond to one phase out of the three.

3.2.2 Tap Transformers and Shunts

The frequency of a transmission system, sometimes called system frequency, is constant throughout the network whereas the voltage is not. The voltage largely depends on the local situation of the system and as a consequence, can only be controlled locally [3]. Tap transformers and shunts are system components that play a very important role in controlling the voltage across the network.

A tap transformer, also called tap-changing transformer is a transformer in which the turns ratio[4] can be adjusted. A mechanical tap is used to adjust the ratio. The voltages on either side of the transformer are related as,

$$|V_2| = \frac{|V_1|}{t}$$

where t is the turns ratio.

As there is a strong relation between reactive power exchange and voltage levels, shunts are used to balance voltage levels by consuming or injecting reactive power. At a network bus, reactive power consumption results in a lower bus voltage and reactive power injection results in a higher bus voltage. Shunt capacitors inject reactive power whereas shunt inductors consume reactive power. A shunt is modelled as a reactance $z_s = jx_s$ between the bus and the ground. The shunt admittance is defined as follows.

$$y_s = \frac{1}{z_s} = -j\frac{1}{x_s} = jb_s$$

For inductive shunts, x_s is positive and for capacitive shunts, x_s is negative. Note that the shunt susceptance is $b_s = -1/x_s$.

[4]Turns ratio is the ratio between number of windings on primary and secondary sides of a transformer.

3.3 The Power Flow Model

As the name implies, power flow or load flow simulations involve understanding the flow of electric power from source to destination. Power flow gives insight about the *state* of the transmission system and is one of the most important network computations. State, also referred to as grid state, describes *steady-state* behavior of the network and is defined by three quantities; power, current and voltage. Steady-state means that only power frequency (50 or 60 Hz) is considered for calculations and the time step could be minutes, hours, months or years[5]. Given power injections at different parts of the network, the objective is to compute voltage at every node and current in every line. We derive power flow equations and define the power flow problem as follows.

At each node i of the network, complex power is defined by,

$$S_i = V_i I_i^* \tag{3.15}$$

where V_i is the potential difference between the node i and ground, and I_i is the current *injected* at node i. From Kirchhoff's Current Law we have,

$$I_i = \sum_{k=1}^{N} I_{ik} \tag{3.16}$$

where I_{ik} is the current between node i and node $k \neq i$. That is, it's the current flowing from every node in the network to node i. From Ohm's law, line current is related to voltage as,

$$I_{ik} = Y_{ik} V_k \tag{3.17}$$

where V_k is the voltage at node[6] k and Y_{ik} is the admittance[7] of the transmission line joining nodes i and k. In matrix form,

$$\mathbf{I} = \mathbf{Y}\mathbf{V} \tag{3.18}$$

where $\mathbf{I} \in \mathbb{C}^N$ is the vector of current injections at nodes, $\mathbf{V} \in \mathbb{C}^N$ is the vector of node voltages and $\mathbf{Y} = [Y_{ik}] \in \mathbb{C}^{N \times N}$ is called *admittance matrix*. The entries $[Y_{ik}]$ define the line impedance between node i and node k. From (3.10) we have, $Y_{ik} = G_{ik} + jB_{ik}$. For nodes not directly connected to node i, $Y_{ik} = 0$ and hence $\mathbf{Y}$ is sparse and in KCL, it is sufficient to sum only over nodes that are *directly* connected to node i.

---

[5]Dynamic(kHz) and transient(MHz) analyses consider milliseconds and microseconds respectively for calculations.

[6]From Ohm's law, V_k should have been the voltage drop across the impedance but we consider it as voltage at node k for now, as we will see further that the potential difference between nodes i and k arises in the power flow equations once we introduce phasors.

[7]It is convenient to use admittance Y instead of impedance Z as we can define the admittance between two unconnected nodes as 0.

Complex power at node i can now be written as,

$$\begin{aligned} S_i &= V_i (YV)_i^* \\ &= V_i \left(\sum_{k=1}^{N} Y_{ik} V_k \right)^* \end{aligned} \tag{3.19}$$

Using phasors and expanding Y_{ik},

$$\begin{aligned} S_i &= \sum_{k=1}^{N} |V_i||V_k| e^{j\delta_{ik}} (G_{ik} - jB_{ik}) \\ &= \sum_{k=1}^{N} |V_i||V_k| \left(\cos \delta_{ik} + j \sin \delta_{ik}\right) \left(G_{ik} - jB_{ik}\right)) \end{aligned}$$

where $\delta_{ik} = (\delta_i - \delta_k)$ denotes the difference in phase angles between node i and k. Considering the real and imaginary terms of complex power S_i, we have the following two equations for active and reactive power which are called *power flow equations*.

$$P_i = \sum_{k=1}^{N} |V_i||V_k| \left(G_{ik} \cos \delta_{ik} + B_{ik} \sin \delta_{ik}\right) \tag{3.20a}$$

$$Q_i = \sum_{k=1}^{N} |V_i||V_k| \left(G_{ik} \sin \delta_{ik} - B_{ik} \cos \delta_{ik}\right) \tag{3.20b}$$

The power flow problem, also called load flow problem can now be stated as:

Given the power injection S at each node,
find the voltage* V *at every node and current* I *in every line.

This problem is solved by computing V from the power flow equations and then computing I using Ohm's law and KCL.

The power flow equations form a system of non-linear equations for which a closed-form solution is not known to exist. However, it is a root-finding problem and we use well established methods such as the Newton Raphson iterative algorithm to find a numerical solution.

Solving the power flow problem is of tremendous importance since it lies at the root of various applications in power system analysis. In this report we focus on the following applications which are relevant to the project.

1. Reactive power compensation: As explained in section 3.2.2, shunts are used to regulate voltages across the transmission network. Reactive power compensation assessment is made to quantify the amount of shunt inductors and capacitors banks needed for voltage regulation in the future.

2. Year-round calculations: Year-round calculations involve evaluating power flow for every hour of the year. The hourly data of supply and demand is fed into the model and the voltages and the currents are analyzed. Year-round calculations give a broad insight into the behavior of the transmission network over long periods of time. In power system planning, year-round calculations are carried out for the coming decades to assess how the existing network needs to be expanded in the future.

3. Contingency analysis: In electricity systems, contingency analysis is an investigation of scenarios wherein system components such as generators or transmission lines are out of service or are taken down for maintenance. A standard criterion in contingency analysis is the N-1 criterion which is often called N-1 secure (for normal minus one). If an electric grid is called N-1 secure, it means that the grid should be functional even if one system component such as a major transmission line is out of service. For higher security, some electric grids are made N-2 secure in which case the grid should be able to withstand two contingencies, that is, the loss of two system components.

Chapter 4

Power Flow Solvers

Digital solution methods to solve the power flow problem first appeared in the literature in 1956 and major breakthroughs in power flow computations were made in the 1960s [8]. There has been a lot of research in numerical methods to efficiently solve the power flow problem ever since. In recent times, considering the rapidly growing sizes of electric grids, power flow solvers are of tremendous importance to power system operators.

Since the performance of a power flow solver depends largely on various factors such as problem size, available computing power and ways of implementation, it is often very hard to choose the right solver for a given problem. In this chapter, we describe some of the most widely used power flow solvers.

4.1 Newton-Raphson

The Newton-Raphson (NR) method is a widely accepted root-finding algorithm that can be used to solve a system of non-linear equations of the form $F(x) = 0$. Starting with an initial approximation, the iterative scheme involves making successive corrections to vector x. The correction vector Δx is assumed to satisfy $F(x+\Delta x) = 0$ at each iteration and a first order Taylor expansion of $F(x + \Delta x)$ gives the NR iterative formula

$$-J(x)\Delta x = F(x) \tag{4.1}$$

where $J(x)$ is the Jacobian matrix calculated as $J_{ik} = \frac{\partial F_i(x)}{\partial x_k}$. The partial derivatives represent the slopes of the tangent hyperplanes [8]. Algorithm (1) describes the basic structure of the Newton-Raphson method. Traditionally, direct solvers are used to solve the Jacobian matrix equation in each iteration. The residual norm $\|F(x^k)\|$ or the relative residual norm $\|\frac{F(x^k)}{F(x^0)}\|$ is used as a measure to check convergence. The Newton-Raphson method is known to have quadratic convergence when iterates are close to the solution [7]. The iteration process of the Newton-Raphson method for a one-dimensional function is shown in fig. 4.1.

Algorithm 1: Newton-Raphson Method

$k := 0$
Initialize: x^0
while *not converged* **do**
  Solve for the correction: $-J(x^k)\Delta x^k = F(x^k)$
  Update the approximation: $x^{k+1} = x^k + \Delta x^k$
  $k = k + 1$
end

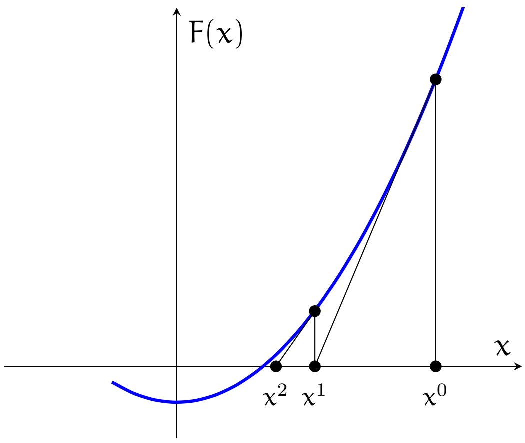

Figure 4.1: Newton-Raphson iterations

The classical approach to initialize x^0 is to use the *flat start* as initial value. That is, all voltage angles are set to 0 and voltage magnitudes are set to 1 pu (equal to that of the slack bus). For better convergence, the solutions of approximate methods such as DC approximation (described in section 4.3) are used as initial values.

To solve the power flow problem using the NR method, $F(x)$ can be formulated as power or current mismatch functions. The unknown variable vector x can be represented in three different coordinates such as polar, Cartesian and complex form as shown in table 4.1.

The two mismatch formulations of $F(x)$ and three coordinate forms of x result in six possible ways of applying the Newton-Raphson method to solve power flow problems. These six methods are considered as the fundamental Newton power flow methods based on which various modified versions are developed [9].

The most widely used version is power-mismatch formulation with polar coordinates which is introduced in [10]. The current-mismatch versions with polar and Cartesian coordinates developed in [9] are found to perform well for large scale transmission sys-

Table 4.1: Variable x in different coordinates

Coordinates	Variable x
Polar $\left(V_i = \|V_i\|e^{j\delta_i}\right)$	$[\delta_1, \ldots, \delta_n, \|V_1\|, \ldots, \|V_n\|]^T$
Cartesian $(V_i = V_i^r + jV_i^m)$	$[V_1^m, \ldots, V_n^m, V_1^r, \ldots, V_n^r]^T$
Complex form (V_i)	$[V_1, \ldots, V_n]^T$

tems. In this report, we review the three versions; polar power-mismatch version introduced in [10], polar and Cartesian current-mismatch versions developed in [9]. For a detailed comparison of NR methods, we refer to [9] where all six versions are investigated with numerical experiments and a general framework for applying NR methods to power flow problems in transmission and distribution systems is presented.

4.1.1 Polar power-mismatch version

The power-mismatch function $F(x)$ is formulated as,

$$\begin{aligned} F_i(x) = \Delta S_i(x) &= S_i^{sp} - S_i(x) \\ &= S_i^{sp} - V_i \sum_{k=1}^{N} Y_{ik}^* V_k^* \end{aligned} \tag{4.2}$$

where $S_i^{sp} = P_i^{sp} + jQ_i^{sp}$ is the specified complex power injection at bus i and $S_i(x)$ is the complex power computed at bus i which follows from (3.19).

In polar coordinates, $\Delta S_i(x)$ is separated using (3.20) as,

$$\Delta P_i(x) = P_i^{sp} - \sum_{k=1}^{N} |V_i||V_k| \left(G_{ik} \cos\delta_{ik} + B_{ik} \sin\delta_{ik}\right) \tag{4.3a}$$

$$\Delta Q_i(x) = Q_i^{sp} - \sum_{k=1}^{N} |V_i||V_k| \left(G_{ik} \sin\delta_{ik} - B_{ik} \cos\delta_{ik}\right) \tag{4.3b}$$

Using the polar power-mismatch function, the Newton-Raphson iterative formula can be written as follows.

$$-\left[\begin{array}{c|c} J^{11} & J^{12} \\ \hline J^{21} & J^{22} \end{array}\right] \left[\begin{array}{c} \Delta\delta \\ \Delta|V| \end{array}\right] = \left[\begin{array}{c} \Delta P \\ \Delta Q \end{array}\right] \tag{4.4}$$

where the Jacobian sub-matrices are defined as $J^{11} = \frac{\partial \Delta P}{\partial \delta}$, $J^{12} = \frac{\partial \Delta P}{\partial |V|}$, $J^{21} = \frac{\partial \Delta Q}{\partial \delta}$, $J^{22} = \frac{\partial \Delta Q}{\partial |V|}$ and the partial derivatives $J_{ik} = \frac{\partial F_i(x)}{\partial x_k}$ are calculated as follows.

$$
\left.
\begin{aligned}
\frac{\partial \Delta P_i(x)}{\partial |V_k|} &= -|V_i|(G_{ik}\cos\delta_{ik} + B_{ik}\sin\delta_{ik}) \\
\frac{\partial \Delta Q_i(x)}{\partial |V_k|} &= -|V_i|(G_{ik}\sin\delta_{ik} - B_{ik}\cos\delta_{ik}) \\
\frac{\partial \Delta P_i(x)}{\partial \delta_k} &= -|V_i||V_k|(G_{ik}\sin\delta_{ik} - B_{ik}\cos\delta_{ik}) \\
\frac{\partial \Delta Q_i(x)}{\partial \delta_k} &= -|V_i||V_k|(-G_{ik}\cos\delta_{ik} - B_{ik}\sin\delta_{ik})
\end{aligned}
\right\} \quad (i \neq k)
$$

$$
\left.
\begin{aligned}
\frac{\partial \Delta P_i(x)}{\partial |V_i|} &= -\left(2|V_i|G_{ii} + \sum_{i\neq k}|V_k|(G_{ik}\cos\delta_{ik} + B_{ik}\sin\delta_{ik})\right) \\
\frac{\partial \Delta Q_i(x)}{\partial |V_i|} &= -\left(-2|V_i|B_{ii} + \sum_{i\neq k}|V_k|(G_{ik}\sin\delta_{ik} - B_{ik}\cos\delta_{ik})\right) \\
\frac{\partial \Delta P_i(x)}{\partial \delta_i} &= -\sum_{i\neq k}|V_i||V_k|(-G_{ik}\sin\delta_{ik} + B_{ik}\cos\delta_{ik}) \\
\frac{\partial \Delta Q_i(x)}{\partial \delta_i} &= -\sum_{i\neq k}|V_i||V_k|(G_{ik}\cos\delta_{ik} + B_{ik}\sin\delta_{ik})
\end{aligned}
\right\} \quad (i = k)
$$

To solve the linear system (4.4), it has to be modified based on the information available at each bus for the following reason. We know from section 3.2.1 that at each PV bus, P and $|V|$ are specified whereas Q and δ are unknown. Hence, for each PV bus j, ΔQ_j cannot be formulated and the corresponding partial derivatives in the Jacobian matrix cannot be computed. As a result, we eliminate the entries $\frac{\partial \Delta P_i}{\partial |V_j|}$, $\frac{\partial \Delta Q_i}{\delta |V_j|}$, $\frac{\partial \Delta Q_j}{\partial |V_i|}$ and $\frac{\partial \Delta Q_j}{\partial \delta_i}$ for all $i = 1 \ldots N$ from the Jacobian matrix $J(x)$, $\Delta|V_j|$ from the correction vector Δx and ΔQ_j from the power mismatch function $F(x)$ for each PV bus j. Similarly, δ and $|V|$ are known for the slack bus and the corresponding entries in the linear system are eliminated. The order of $J(x)$ reduces to $(2N - N_g - 2)$ and the vector x becomes,

$$
x = \left[\delta_2, \ldots, \delta_N, |V_{N_g+2}|, \ldots, |V_N|\right]^T
$$

Note that conventionally, δ_1 and $|V_1|$ correspond to the slack bus. The modified linear system is solved at each NR iteration.

4.1.2 Polar current-mismatch version

The current-mismatch function is formulated using the current equation (3.16) and the complex power equation (3.15) as follows.

$$
\begin{aligned}
F_i(x) = \Delta I_i(x) &= I_i^{sp} - I_i(x) \\
&= \left(\frac{S_i^{sp}}{V_i}\right)^* - \sum_{k=1}^{N} Y_{ik} V_k
\end{aligned} \tag{4.5}
$$

where $I_i^{sp} = \left(\frac{S_i^{sp}}{V_i}\right)^*$ is the complex current injection specified at bus i and $I_i(x)$ is the complex current computed at bus i.

The function $\Delta I_i(x)$ is separated into real $\Delta I_i^r(x)$ and imaginary $\Delta I_i^m(x)$ current-mismatch functions in polar form as follows.

$$
\Delta I_i^r(x) = \frac{P_i^{sp}\cos\delta_i + Q_i^{sp}\sin\delta_i}{|V_i|} - \sum_{k=1}^{N} |V_k| \left(G_{ik}\cos\delta_k - B_{ik}\sin\delta_k\right) \tag{4.6a}
$$

$$
\Delta I_i^m(x) = \frac{P_i^{sp}\sin\delta_i - Q_i^{sp}\cos\delta_i}{|V_i|} - \sum_{k=1}^{N} |V_k| \left(G_{ik}\sin\delta_k + B_{ik}\cos\delta_k\right) \tag{4.6b}
$$

The NR iterative formula for the polar current-mismatch version can be written as,

$$
-\left[\begin{array}{c|c} J^{11} & J^{12} \\ \hline J^{21} & J^{22} \end{array}\right] \left[\begin{array}{c} \Delta\delta \\ \Delta|V| \end{array}\right] = \left[\begin{array}{c} \Delta I^r \\ \Delta I^m \end{array}\right] \tag{4.7}
$$

where $J^{11} = \frac{\partial \Delta I^r}{\partial \delta}$, $J^{12} = \frac{\partial \Delta I^r}{\partial |V|}$, $J^{21} = \frac{\partial \Delta I^m}{\partial \delta}$, and $J^{22} = \frac{\partial \Delta I^m}{\partial |V|}$. The partial derivatives are calculated as follows.

$$
\left.
\begin{aligned}
\frac{\partial \Delta I_i^r(x)}{\partial |V_k|} &= -(G_{ik}\cos\delta_k - B_{ik}\sin\delta_k) \\
\frac{\partial \Delta I_i^m(x)}{\partial |V_k|} &= -(G_{ik}\sin\delta_k + B_{ik}\cos\delta_k) \\
\frac{\partial \Delta I_i^r(x)}{\partial \delta_k} &= |V_k|(G_{ik}\sin\delta_k + B_{ik}\cos\delta_k) \\
\frac{\partial \Delta I_i^m(x)}{\partial \delta_k} &= -|V_k|(G_{ik}\cos\delta_k - B_{ik}\sin\delta_k)
\end{aligned}
\right. \qquad (i \neq k)
$$

$$
\left.
\begin{aligned}
\frac{\partial \Delta I_i^r(x)}{\partial |V_i|} &= -\left(G_{ii}\cos\delta_i - B_{ii}\sin\delta_i\right) - \frac{P_i^{sp}\cos\delta_i + Q_i^{sp}\sin\delta_i}{|V_i|^2} \\
\frac{\partial \Delta I_i^m(x)}{\partial |V_i|} &= -\left(G_{ii}\sin\delta_i + B_{ii}\cos\delta_i\right) - \frac{P_i^{sp}\sin\delta_i - Q_i^{sp}\cos\delta_i}{|V_i|^2} \\
\frac{\partial \Delta I_i^r(x)}{\partial \delta_i} &= |V_i|\left(G_{ii}\sin\delta_i + B_{ii}\cos\delta_i\right) - \frac{P_i^{sp}\sin\delta_i - Q_i^{sp}\cos\delta_i}{|V_i|} \\
\frac{\partial \Delta I_i^m(x)}{\partial \delta_i} &= -|V_i|\left(G_{ii}\cos\delta_i - B_{ii}\sin\delta_i\right) + \frac{P_i^{sp}\cos\delta_i + Q_i^{sp}\sin\delta_i}{|V_i|}
\end{aligned}
\right. \qquad (i = k)
$$

Similar to power-mismatch version, the linear system (4.7) has to be modified. For a PQ bus, computation of real and imaginary current-mismatch functions is straightforward since the associated real and reactive power mismatches are known. Whereas representing a PV bus in the linear system is tricky and there are several approaches available in literature. In this report, we review the new approach developed in [9] which is found to be promising.

For each PV bus j, the reactive power Q_j is considered as a dependent variable of $|V|$ and δ. The current-mismatch formulation is directly used. That is, $\Delta I_i^r(x)$ and $\Delta I_i^m(x)$ are calculated using $Q_i^{sp} = Q_j$ in equations (4.6) for each PV bus j at each iteration. The partial derivatives $\frac{\partial \Delta I_i^r}{\partial |V_j|}$ and $\frac{\partial \Delta I_i^m}{\partial |V_j|}$ in the Jacobian matrix $J(x)$ are replaced by $\frac{\partial \Delta I_i^r}{\partial Q_j}$ and $\frac{\partial \Delta I_i^m}{\partial Q_j}$ for all $i = 1 \ldots N$ which are calculated as follows.

$$\begin{aligned} \frac{\partial \Delta I_i^r(x)}{\partial Q_j} &= 0 \\ \frac{\partial \Delta I_i^m(x)}{\partial Q_j} &= 0 \end{aligned} \qquad (i \neq j)$$

$$\begin{aligned} \frac{\partial \Delta I_j^r(x)}{\partial Q_j} &= \frac{\sin \delta_j}{|V_j|^{sp}} \\ \frac{\partial \Delta I_j^r(x)}{\partial Q_j} &= -\frac{\cos \delta_j}{|V_j|^{sp}} \end{aligned} \qquad (i = j)$$

The entries $\Delta|V_j|$ in the correction vector Δx are replaced by ΔQ_j for each PV bus j. The initial reactive power Q_j^0 is calculated for each PV bus j as follows.

$$Q_j^0 = \sum_{k=1}^{N} |V_j||V_k| \left(G_{jk} \sin \delta_{jk} - B_{jk} \cos \delta_{jk}\right)$$

The order of $J(x)$ remains $(2N - 2)$. At each NR iteration, the modified linear system is solved and the reactive power Q_j is updated using the computed correction ΔQ_j.

4.1.3 Cartesian current-mismatch version

In Cartesian form, the current-mismatch function $F(x)$ is separated as,

$$\Delta I_i^r(x) = \frac{P_i^{sp} V_i^r + Q_i^{sp} V_i^m}{(V_i^r)^2 + (V_i^m)^2} - \sum_{k=1}^{N} \left(G_{ik} V_k^r - B_{ik} V_k^m\right) \tag{4.8a}$$

$$\Delta I_i^m(x) = \frac{P_i^{sp} V_i^m - Q_i^{sp} V_i^r}{(V_i^r)^2 + (V_i^m)^2} - \sum_{k=1}^{N} \left(G_{ik} V_k^m + B_{ik} V_k^r\right) \tag{4.8b}$$

and the Jacobian matrix equation is formulated as follows.

$$-\left[\begin{array}{c|c} J^{11} & J^{12} \\ \hline J^{21} & J^{22} \end{array}\right]\left[\begin{array}{c} \Delta V^{m} \\ \Delta V^{r} \end{array}\right]=\left[\begin{array}{c} \Delta I^{r} \\ \Delta I^{m} \end{array}\right] \tag{4.9}$$

where $J^{11}=\frac{\partial \Delta I^{r}}{\partial V^{m}}$, $J^{12}=\frac{\partial \Delta I^{r}}{\partial V^{r}}$, $J^{21}=\frac{\partial \Delta I^{m}}{\partial V^{m}}$, and $J^{22}=\frac{\partial \Delta I^{m}}{\partial V^{r}}$. The partial derivatives are computed as,

$$\begin{aligned} \frac{\partial \Delta I_i^r(x)}{\partial V_k^r} &= -G_{ik} \\ \frac{\partial \Delta I_i^m(x)}{\partial V_k^r} &= B_{ik} \\ \frac{\partial \Delta I_i^r(x)}{\partial V_k^m} &= B_{ik} \\ \frac{\partial \Delta I_i^m(x)}{\partial V_k^m} &= -G_{ik} \end{aligned} \qquad (i \neq k)$$

$$\begin{aligned} \frac{\partial \Delta I_i^r(x)}{\partial V_i^r} &= -G_{ii} - \frac{P_i^{sp}\left((V_i^r)^2-(V_i^m)^2\right)+2V_i^rV_i^mQ_i^{sp}}{|V_i|^4} \\ \frac{\partial \Delta I_i^m(x)}{\partial V_i^r} &= -B_{ii} + \frac{Q_i^{sp}\left((V_i^r)^2-(V_i^m)^2\right)-2V_i^rV_i^mP_i^{sp}}{|V_i|^4} \\ \frac{\partial \Delta I_i^r(x)}{\partial V_i^m} &= B_{ii} + \frac{Q_i^{sp}\left((V_i^r)^2-(V_i^m)^2\right)-2V_i^rV_i^mP_i^{sp}}{|V_i|^4} \\ \frac{\partial \Delta I_i^m(x)}{\partial V_i^m} &= -G_{ii} + \frac{P_i^{sp}\left((V_i^r)^2-(V_i^m)^2\right)+2V_i^rV_i^mQ_i^{sp}}{|V_i|^4} \end{aligned} \qquad (i = k)$$

In [9], the reactive power Q_j is chosen as a dependent variable to represent a PV bus, similar to polar current-mismatch version. The partial derivatives $\frac{\partial \Delta I_i^r}{\partial Q_j}$ and $\frac{\partial \Delta I_i^m}{\partial Q_j}$ computed as,

$$\begin{aligned} \frac{\partial \Delta I_i^r(x)}{\partial Q_j} &= 0 \\ \frac{\partial \Delta I_i^m(x)}{\partial Q_j} &= 0 \end{aligned} \qquad (i \neq j)$$

$$\begin{aligned} \frac{\partial \Delta I_j^r(x)}{\partial Q_j} &= \frac{V_j^m}{(V_j^r)^2+(V_j^m)^2} \\ \frac{\partial \Delta I_j^r(x)}{\partial Q_j} &= \frac{-V_j^r}{(V_j^r)^2+(V_j^m)^2} \end{aligned} \qquad (i = j)$$

are added to the Jacobian matrix $J(x)$ and the correction ΔQ_j is added to the correction vector Δx for each PV bus j. As a result, the Jacobian matrix becomes a rectangular matrix. That is, $J(x) \in \mathbb{R}^{(2N)\times(2N+N_g)}$. In order to make the Jacobian matrix square, the equation

$$\Delta|V| = \frac{V^r}{|V|}\Delta V^r + \frac{V^m}{|V|}\Delta V^m$$

is used with $\Delta|V_j| = 0$ since $|V_j|$ is specified for each PV bus j. This gives the relation,

$$\Delta V_j^r = -\frac{V_j^m}{V_j^r}\Delta V_j^m$$

which is used to add the column of the Jacobian matrix corresponding to the derivatives $\frac{\partial \Delta I_i^r}{\partial V_j^r}$ and $\frac{\partial \Delta I_i^m}{\partial V_j^r}$ to the column corresponding to the derivatives $\frac{\partial \Delta I_i^r}{\partial V_j^m}$ and $\frac{\partial \Delta I_i^m}{\partial V_j^m}$ as follows.

$$\frac{\partial \Delta I_i^r}{\partial V_j^m}\Delta V_j^m = \left(\frac{\partial \Delta I_i^r}{\partial V_j^m} - \frac{V_j^m}{V_j^r}\frac{\partial \Delta I_i^r}{\partial V_j^r}\right)\Delta V_j^m$$

$$\frac{\partial \Delta I_i^m}{\partial V_j^m}\Delta V_j^m = \left(\frac{\partial \Delta I_i^m}{\partial V_j^m} - \frac{V_j^m}{V_j^r}\frac{\partial \Delta I_i^m}{\partial V_j^r}\right)\Delta V_j^m$$

The correction vector ΔV_j^r is now eliminated from the correction vector Δx for each PV bus j. The initial reactive power Q_j^0 is calculated for each PV bus j as follows.

$$Q_j^0 = \sum_{k=1}^{N}\left(V_j^m\left(G_{jk}V_k^r - B_{jk}V_k^m\right) - V_j^r\left(B_{jk}V_k^r + G_{jk}V_k^m\right)\right)$$

With the slack bus included, the order of $J(x)$ remains $(2N-2)$. At each NR iteration, the modified linear system is solved and the reactive power Q_j is updated using the computed correction ΔQ_j.

Despite its widespread popularity, a drawback the Newton-Raphson method has is computational complexity. The Jacobian matrix has to be computed in every iteration as it depends on the current approximation of the solution. Which means, there is a new linear system (4.1) in every iteration for the algorithm to solve. This makes the solution process computationally bound, particularly for applications such as contingency analysis of large networks. These difficulties in solving the AC power flow problem have led to extensive numerical studies and various simplified methods have been proposed and used. The simplified methods involve making a series of approximations to the nonlinear powerflow problem (3.20). More the approximations made, the easier it is to find a solution. However, note that the AC power flow methods such as Newton-Raphson and all the approximate methods attempt to solve the same underlying power system. In this report, we review two methods that are commonly found in literature: decoupled load flow and dc approximation. In situations where a full power flow model is an absolute necessity, the solutions of these simplified methods are used as initial values, essentially when it is quite certain that the flat start approximation doesn't converge.

4.2 Fast Decoupled Load Flow

The Fast Decoupled Load Flow (FDLF) method is a simple and fast power flow solution technique which is derived from Newton's method. We briefly describe the basic version of the formulation here and refer to [3, 11] for further details.

The polar power-mismatch version of the Newton-Raphson method described in section 4.1.1 is used as a starting point to derive the decoupled load flow formulation. The linear system that is solved in every iteration of the NR polar power-mismatch version is given by (4.1) as,

$$-\left[\begin{array}{c|c} J^{11} & J^{12} \\ \hline J^{21} & J^{22} \end{array}\right]\left[\begin{array}{c} \Delta\delta \\ \Delta|V| \end{array}\right]=\left[\begin{array}{c} \Delta P \\ \Delta Q \end{array}\right] \tag{4.10}$$

The decoupling principle involves making the following assumptions which generally hold for power systems under normal operating conditions [3].

1. Voltage angle differences between buses are small.

$$\cos\delta_{ik} \approx 1; \quad \sin\delta_{ik} \approx \delta_{ik}$$

2. Transmission line susceptances are much larger than conductances.

$$G_{ik}\sin\delta_{ik} \ll B_{ik}$$

3. The reactive power injected into a node is much smaller than the reactive flow that would result if all lines connected to that bus were short circuited to reference [3].

$$Q_i \ll B_{ii}|V_i|^2$$

Evaluating the partial derivatives $J^{12} = \frac{\partial\Delta P}{\partial|V|}$ and $J^{21} = \frac{\partial\Delta Q}{\partial\delta}$ (see section 4.1.1 for equations) with the first two assumptions shows that the Jacobian sub-matrices J^{12} and J^{21} are small and can be neglected. Additionally, the terms $[J^{22}_{ik}]$ are multiplied with voltage magnitude $|V_i|$, the convenience of which will be clear in the derivation below. The following decoupled system of equations is then obtained.

$$-\left[\ J^{11}\ \right]\left[\ \Delta\delta\ \right]=\left[\ \Delta P\ \right] \tag{4.11a}$$

$$-\left[\ \widetilde{J}^{22}\ \right]\left[\ \Delta|\widetilde{V}|\ \right]=\left[\ \Delta Q\ \right] \tag{4.11b}$$

where, $J^{11}_{ik} = \frac{\partial\Delta P_i}{\partial\delta_k}$, $\widetilde{J}^{22}_{ik} = |V_i|\frac{\partial\Delta Q_i}{\partial|V_k|}$ and $\Delta|\widetilde{V}_i| = \frac{\Delta|V_i|}{|V_i|}$. The Jacobian sub-matrices J^{11} and $\widetilde{J}^{22}$ are computed using the partial derivatives defined in section 4.1.1 with the three assumptions stated above as follows.

$$\frac{\partial \Delta P_i}{\partial \delta_k} = |V_i| \frac{\partial \Delta Q_i}{\partial |V_k|} = -|V_i||V_k| \left(G_{ik} \sin \delta_{ik} - B_{ik} \cos \delta_{ik} \right) \qquad (i \neq k)$$
$$\approx |V_i||V_k| B_{ik}$$

$$\begin{aligned} \frac{\partial \Delta P_i}{\partial \delta_i} &= \sum_{i \neq k} |V_i||V_k| (G_{ik} \sin \delta_{ik} - B_{ik} \cos \delta_{ik}) \qquad (i = k) \\ &= B_{ii}|V_i|^2 + \sum_{k=1}^{N} |V_i||V_k| \left(G_{ik} \sin \delta_{ik} - B_{ik} \cos \delta_{ik} \right) \\ &= B_{ii}|V_i|^2 + Q_i \\ &\approx B_{ii}|V_i|^2 \end{aligned}$$

$$\begin{aligned} |V_i| \frac{\partial \Delta Q_i}{\partial |V_i|} &= 2B_{ii}|V_i|^2 - \sum_{i \neq k} |V_i||V_k| (G_{ik} \sin \delta_{ik} - B_{ik} \cos \delta_{ik}) \quad (i = k) \\ &= B_{ii}|V_i|^2 - Q_i \\ &\approx B_{ii}|V_i|^2 \end{aligned}$$

The decoupled system (4.11) is now written as,

$$-\left[\; |V|^T B |V| \; \right] \left[\; \Delta\delta \; \right] = \left[\; \Delta P \; \right]$$

$$-\left[\; |V|^T B |V| \; \right] \left[\; \Delta|\widetilde{V}| \; \right] = \left[\; \Delta Q \; \right]$$

where $B = [B_{ik}] \in \mathbb{R}^{N \times N}$ is the matrix of line susceptances. Finally, the terms $|V_i|^T$ are taken to the right hand side and the terms $|V_i|$ are set to 1 pu. A distinction is made at this stage for matrix B in the two linear systems for convenience.

With all the above modifications, the final decoupled power flow equations become,

$$-\left[\; B' \; \right] \left[\; \Delta\delta \; \right] = \left[\; \Delta\widetilde{P} \; \right] \tag{4.12a}$$

$$-\left[\; B'' \; \right] \left[\; \Delta|V| \; \right] = \left[\; \Delta\widetilde{Q} \; \right] \tag{4.12b}$$

where $\Delta\widetilde{P}_i = \frac{\Delta P_i}{|V_i|}$ and $\Delta\widetilde{Q}_i = \frac{\Delta Q_i}{|V_i|}$. The decoupled system (4.12) is modified to represent a PV bus, similar to NR polar power-mismatch version as described in section 4.1.1. The order of the systems (4.12) will then be $(N-1)$ and $(N-N_g-1)$ respectively.

The matrices B' and B'' depend only on network parameters and are constant in every iteration. This means that the matrices have to be calculated and factorized only once, leading to faster computations of the power flow problem even though the number of iterations needed for convergence could be higher because of the approximations made. The steps involved in the fast decoupled load flow method are given in the following algorithm.

Algorithm 2: Decoupled load flow

$k := 0$
Initialize: δ^0 and $|V|^0$
while *not converged* **do**
  Compute: $\Delta\widetilde{P}$
  Solve for the correction $\Delta\delta$: $-[B'][\Delta\delta] = [\Delta\widetilde{P}]$
  Update the approximation: $\delta^{k+1} = \delta^k + \Delta\delta^k$
  Use δ^{k+1} to compute $\Delta\widetilde{Q}$
  Solve for the correction $\Delta|V|$: $-[B''][\Delta|V|] = [\Delta\widetilde{Q}]$
  Update the approximation: $|V|^{k+1} = |V|^k + \Delta|V|^k$
  $k = k + 1$
end

4.3 DC approximation

DC approximation or DC load flow is a linear approximation of the power flow problem. The extent to which the non-linear power flow equations (3.20) are approximated and the kinds of assumptions made may vary based on the problem or the application. In fact, 'DC' refers to the collection of approximations made such that the network is *decoupled*. In some cases, the FDLF method is also considered as a DC approximation method. However, there is a fundamental difference between FDLF and DC approximation methods. In FDLF, the non-linear system is solved in each iteration and the approximation is made only to the Jacobian matrix. In DC load flow methods, the non-linear equations are linearized to speed up computation, which considerably affects the accuracy of the final solution.

The DC load flow method described in [3] is derived as follows. The following approximations are made to the power flow problem (3.20).

- Bus voltage magnitudes are set to 1 pu in active power equations (3.20a).
- Voltage magnitudes are approximated as: $|V| = 1 + \Delta|V|$ and $\frac{1}{1+\Delta|V|} = 1 - \Delta|V|$ in reactive power equations (3.20b).
- Conductances of transmission lines are neglected: $G_{ik} \ll B_{ik}$.
- Voltage angles are small: $\cos\delta_{ik} \approx 1$ and $\sin\delta_{ik} \approx \delta_{ik}$.

Under these assumptions, the linearized version of the power flow problem (3.20) is given by,

$$P_i = \sum_{k \neq i} B_{ik} \delta_{ik} \tag{4.13a}$$

$$Q_i + B_{ii} = (Q_i - B_{ii}) \Delta |V_i| + \sum_{k \neq i} (1 + \Delta |V_k|) B_{ik} \tag{4.13b}$$

where $\Delta|V|$ represents the deviation of the voltage magnitude from 1 pu voltage level.

The DC approach provides a fairly good approximation of voltage magnitudes and angles which can be used as initial values in NR or FDLF methods. It is also claimed in [12] that while the DC approximation leads to some loss of accuracy, the results match fairly closely with full power flow solution. The following approach of DC approximation is presented in [12] as the most dramatic of DC approximation methods.

The assumptions made to the non-linear power flow problem are:

- the reactive power balance equations are ignored,
- voltage magnitudes are set to 1 pu,
- line losses are ignored.

These assumptions reduce the non-linear power flow problem to the system of linear equations:

$$[B'] \, [\delta] = [P] \tag{4.14}$$

where $[B']$ is the line susceptance matrix, $[\delta]$ is the vector of bus voltage angles and $[P]$ is the active power injection vector.

It should be noted that the lack of losses in the DC solution can be reasonably compensated for by increasing the total load by the amount of estimated losses. The DC approach (4.14) has the following significant advantages over the Newton-Raphson method.

1. The linear system is half the size of the full problem since only the active power mismatch equations are solved.
2. The algorithm is not iterative, requiring just one single solution of (4.14).
3. The matrix B' is dependent only on network parameters and needs to be factorized only once.

We refer to [12] for further details, where a comparison between AC and DC methods is also made.

4.4 Gauss-Seidel

Gauss-Seidel method is another iterative technique that can be used to solve the non-linear power flow problem. The iterative scheme is derived from the complex power equation (3.19) with complex voltage V_i as the iteration variable.

$$\begin{aligned} S_i &= V_i (YV)_i^* \\ &= V_i \left(\sum_{k=1}^{N} Y_{ik} V_k \right)^* \\ &= V_i \left(\sum_{k \neq i} Y_{ik} V_k \right)^* + V_i Y_{ii}^* V_i^* \quad \Longleftrightarrow \\ V_i Y_{ii}^* V_i^* &= S_i - V_i \left(\sum_{k \neq i} Y_{ik} V_k \right)^* \quad \Longleftrightarrow \\ V_i^* &= \frac{1}{Y_{ii}^*} \left(\frac{S_i}{V_i} - \sum_{k \neq i} Y_{ik}^* V_k^* \right) \quad \Longleftrightarrow \\ V_i &= \frac{1}{Y_{ii}} \left(\frac{S_i^*}{V_i^*} - \sum_{k \neq i} Y_{ik} V_k \right) \\ &= \frac{1}{Y_{ii}} \left(\frac{P_i - jQ_i}{V_i^*} - \sum_{k \neq i} Y_{ik} V_k \right) \end{aligned} \tag{4.15}$$

The fixed point equation (4.15) leads to the following iterative formula.

$$V_i^{h+1} = \frac{1}{Y_{ii}} \left(\frac{P_i - jQ_i}{V_i^{h*}} - \sum_{k \neq i} Y_{ik} V_k^h \right), \quad h = 0, 1, 2, \ldots \tag{4.16}$$

where V_i^0 is a given initial approximation for each bus i. Equation (4.16) is evaluated at each iteration until convergence is met. If the approximations V_i^h are computed at once for all buses and applied at once in the next iteration, the iterative procedure is called *Jacobi* iteration. If the approximations are computed for one bus at a time and immediately used in the same iteration, the procedure is referred to as *Gauss-Seidel* iteration.

For a PQ bus, it is straightforward to apply the iterative formula (4.16), whereas for a PV bus, modifications are required, similar to Newton-Raphson method.

The Gauss-Seidel method is flexible and relatively easy to implement but it is generally slow and inefficient for large systems. The iterative scheme has a tendency to use a lot of computations, particularly in large scale problems, and could also converge to incorrect solutions. Hence, the Gauss-Seidel method is not preferred in practice. However, despite the shortcomings, it can be used to get a good perspective on power flow problems [13].

4.5 Summary

The following can be inferred from the power flow solvers that are described in the preceding sections (4.1 to 4.4).

- The **Newton-Raphson** method is widely regarded as the most commonly preferred power flow solver [8]. Several formulations of the NR method are found in literature. Among the six fundamental NR methods, the most widely used version is the power-mismatch formulation with polar coordinates [10]. The current-mismatch version with polar and Cartesian coordinates are found to give the best results for transmission networks [9].

- The **Gauss-Seidel** method is another full power flow solver that is used in power flow analysis. Despite the ease of implementation that the Gauss-Seidel method offers, it is seldom preferred in practice due to computational intensity [13].

- The **FDLF** method offers computational benefits against full power flow solvers by making approximations as described in section 4.2. The FDLF method is advantageous in terms of speed and simplicity compared to full power flow solvers [11]. However, the accuracy of the solution is not on par with full power flow solvers because of the approximations made.

- The **DC approximation** method is the simplest of approximate methods to solve the power flow problem. It has been concluded in [12] that the results of the DC approximation method match fairly closely with full power flow solvers despite the loss in accuracy. However, the DC approach considers only active power equations and hence can only substitute a full power flow solver for applications that do not require reactive power to be taken into account.

We would like to emphasize that the selection of a power flow solver is largely problem specific. For instance, while the DC approximation method is well suited for problems that are not sensitive to the approximations made, it cannot be used for applications that require calculation of reactive power in the network. Full power flow solvers such as the Newton-Raphson method and its formulations are always necessary for AC power flow analysis. Hence, for reactive power compensation assessment, AC power flow simulations are absolutely necessary whereas for capacity planning, the DC approach *could* result in a fair approximation.

In the remainder of this section, we investigate the convergence properties of the Newton-Raphson method and evaluate the differences between AC and DC approaches of solving the power flow problem.

Power flow convergence

Mathematically, we call a problem *well-posed* if the following conditions hold.

1. Existence: There exists at least one solution.
2. Uniqueness: There is at most one solution.
3. Stability: The solution depends continuously on input data.

A problem which is not well-posed is called *ill-posed*. Figure 4.2 shows ill-posedness of three one dimensional functions. In power flow analysis, the power flow problem could be ill-posed due to any of the following reasons.

- The system might not have a solution. For example, in fig. 4.2a, $f(x)$ never crosses the x - axis, hence it has no solution.
- Even though a solution exists, the power flow solver cannot find it or convergence is very difficult. For example, fig. 4.2b shows the tendency to diverge when the initial value x_1 is far from the solution. It is clear that $x_3 > x_1$ and continuing the iteration further from x_3 causes the solution to diverge.
- The system might have multiple solutions. For example, in fig. 4.2c, $f(x)$ crosses the x - axis twice, leading to two solutions. For power flow problems, the practical consequence of this is that the solution may converge to a lower voltage value.

Many formulations of the power flow solution methods are available in the literature to fix ill-posedness of power flow problems. These formulations are found to be highly efficient in ensuring convergence and they also help to determine the existence of a solution. In this report we describe the optimal multiplier method as presented in [14] and the line search method of finding the optimal multipliers as explained in [15].

Optimal multiplier method: The Newton-Raphson method has *local* quadratic convergence as mentioned in section 4.1. That is, the NR method converges quadratically when the initial value is close to the solution. A method that converges for any initial value is called *globally* convergent. The optimal multiplier method ensures global convergence and aims to solve the problems of false divergence and convergence to incorrect solutions of the NR method. The optimal multiplier method is popularly known as the *Iwamoto multiplier* method. The core idea is that a scalar multiplier μ is introduced in the update step $x^{k+1} = x^k + \Delta x^k$ of the NR method (see algorithm 1) as follows.

$$x^{k+1} = x^k + \mu \Delta x^k$$

Many studies have been carried out in order to determine the optimal multiplier μ^*. In [14], μ^* is determined as follows.

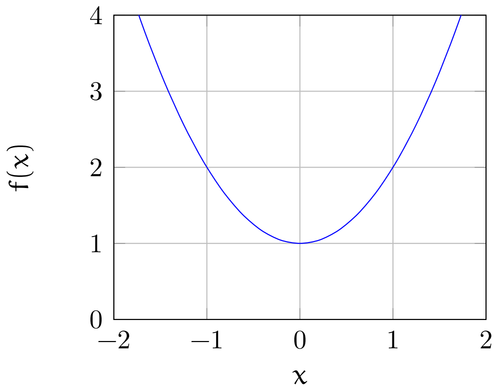

(a) No solution

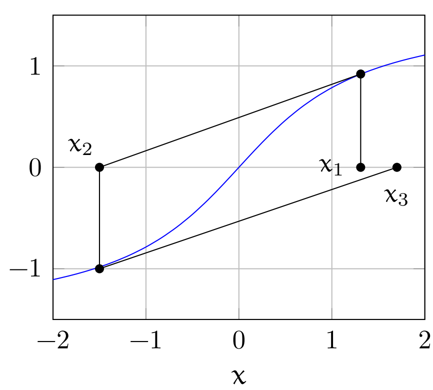

(b) Divergence

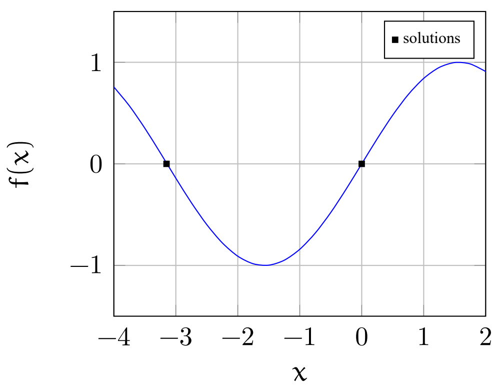

(c) Multiple solutions

Figure 4.2: Ill-posedness

In the Newton-Raphson method, the first order Taylor expansion of the mismatch function $F(x)$ is expressed as (see section 4.1),

$$F(x + \Delta x) = F(x) + J(x)\Delta x = 0$$

where the higher order terms of the expansion are neglected. In [14], the higher order terms are collectively expressed as the mismatch function evaluated at the correction Δx. That is,

$$F(x + \Delta x) = F(x) + J(x)\Delta x + F(\Delta x) = 0$$

Incorporating the multiplier μ,

$$F(x + \mu\Delta x) = F(x) + \mu J(x)\Delta x + \mu^2 F(\Delta x) = 0$$

A cost function $C : \mathbb{R}^n \to \mathbb{R}$ which represents the proximity of the approximation to the solution defined as,

$$C(x) = \frac{1}{2}F(x)^T F(x) \tag{4.17}$$

is used to determine the optimal value of μ by evaluating the following expression.

$$\frac{dC}{d\mu} = 0$$

Algorithm 3 describes the modified Newton-Raphson algorithm with the optimal multiplier incorporated.

Algorithm 3: NR algorithm with optimal multiplier

$k := 0$
Initialize: x^0
while *not converged* **do**
  Solve for the correction: $-J(x^k)\Delta x^k = F(x^k)$
  Compute μ^k by evaluating $\frac{dC}{d\mu} = 0$ •
  Set $\Delta x^k = \mu^k \Delta x^k$ •
  Update the approximation: $x^{k+1} = x^k + \Delta x^k$
  $k = k + 1$
end

Line search technique: To determine the optimal multiplier μ, the line search method is used in [15]. The line search is an iterative method to find a local minimum x^* of an objective function $f : \mathbb{R}^n \rightarrow \mathbb{R}$. In our case, at each iteration the following optimization problem is solved to determine μ^*.

$$\min_{\mu \in [0,1]} C(x^k + \mu \Delta x^k)$$

Since $C(x)$ represents the proximity of the approximation to the solution, the scalar multiplier μ must satisfy $C(x^k + \mu \Delta x^k) < C(x^k)$ at each iteration. Hence, the search is limited to $\mu \in [0, 1]$. The line search procedure is described as follows.

The procedure is similar to the binary search algorithm and starts with $[\mu_1, \mu_2] = [0, 1]$. The domain is then divided in half. That is, $[\mu_1, \mu_3, \mu_2] = [0, 0.5, 1]$. The function $C(x)$ is evaluated at the three points and the following conditions are checked.

$$C(\mu_1) > C(\mu_3)$$
$$C(\mu_2) > C(\mu_3)$$

- If the conditions hold true, the two subdomains $[0, 0.5]$ and $[0.5, 1]$ are further divided in half and the procedure is continued with $[\mu_4, \mu_3, \mu_5] = [0.25, 0.5, 0.75]$ and so on (see fig. 4.3a).
- If one of the conditions is violated, the corresponding subdomain is excluded and the procedure is continued. That is, if $C(\mu_2) < C(\mu_3)$, the three points will be $[\mu_3, \mu_4, \mu_2]$ where μ_4 is the point at the center of $[\mu_3, \mu_2]$ (see fig. 4.3b).

- The procedure terminates when the search domain converges to a point, which is the optimal multiplier μ^*.

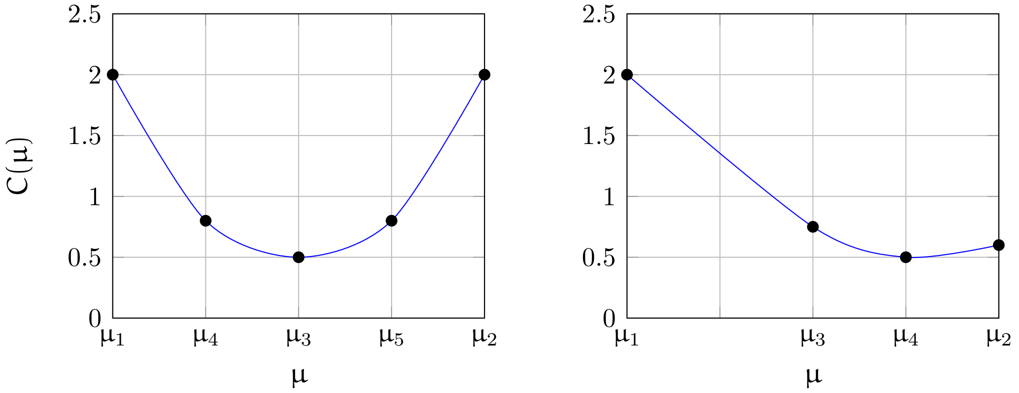

(a) (b)

Figure 4.3: Line search: subdividing the search domains

AC vs DC approach

The benefits of the DC approximation method such as simplicity and computational advantage over full power flow methods are well justified only when the assumptions made in the DC approach are realistic. In [16], the assumptions of the DC power flow method are analyzed and quantified using indices. Here we describe the main ideas in brief.

The assumptions made in the DC approximation method and their respective decisive factors that can be used to judge the accuracy of the DC solution are described as follows.

1. Small voltage angles: $\cos \delta_{ik} \approx 1$ and $\sin \delta_{ik} \approx \delta_{ik}$.
   These assumptions are often said to be useful only for weakly loaded networks. However, if the voltage angles are actually small, this approximation does not lead to significant errors. This is confirmed in [16] with an experiment conducted on the Belgian high voltage grid consisting of about 900 lines and 700 buses with voltages from 70 kV to 380 kV and a peak load of 13 GW. The voltage angle differences were found to be below 7°. In 94% of the lines, the voltage angle differences were found to be lower than 2°. Fig. 4.4 shows the relative error in active power as a consequence of the assumptions made to voltage angles. The relative error is calculated as follows.

$$P_{error} = \frac{P_{ac} - P_{dc}}{P_{ac}} \times 100$$

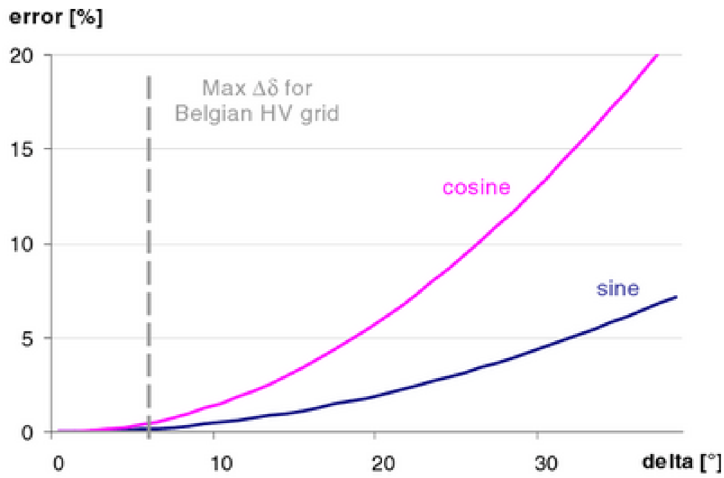

Figure 4.4: Effects of voltage angle approximations

2. Negligible line resistance: $R \ll X$
   In actual electricity networks, it is almost impossible to neglect line resistances. In order to understand the consequences of this assumption, the ratio of reactance to resistance X/R is used as a measure. In [16], it has been shown that an X/R ratio higher than 4 guarantees that the error in active power will be lesser than 5%.

3. Flat voltage profile: All voltage magnitudes are set to 1 pu.
   The deviations of voltages from the assumed value (1 pu) is considered as the decisive factor to assess the effects of the assumption. The voltage deviations are measured by means of standard deviation using the following expression.

$$S_V = \sqrt{\frac{1}{n-1}\sum_{i=1}^{n}(V_i - \overline{V})^2}$$

   The Belgian high voltage network mentioned earlier is taken as an example in [16] to check the likelihood of a favorable voltage profile. It has been found that P_{error} is very sensitive to voltage deviations. Examples of voltages in actual power systems have shown that the assumption of a flat voltage profile is the most critical one and it is the biggest source of P_{error}. Hence, the flat voltage profile is considered to be of high importance for the solution accuracy of the DC approximation method. Flat voltage profile means that the standard deviation of voltages is lesser than 0.01.

It is to be noted that the analyses of the assumptions 1 and 3 made in [16] are case specific and can be considered for reference only when the actual phase angles and voltages of the network are known. Whereas the decisive factor of assumption 2 can be used to check the feasibility of the DC load flow method in all cases since resistances and reactances are characteristics of the network and are always known.

Chapter 5

Software Packages

Given the importance of digital solution methods to power flow analysis, there are many commercial software packages available in the market. These software packages are quite powerful and they are extensively used in the industry for power system operation, control and planning among many other applications. In this chapter we explore PowerFactory, PSS®E and pandapower and understand their capability to solve the power flow problem.

5.1 PowerFactory

PowerFactory is an engineering tool for the analysis of transmission, distribution and industrial electrical power systems. It is designed as an advanced integrated and interactive software package dedicated to electrical power systems in order to achieve the main objectives of planning and operation optimization. PowerFactory has a single-line graphical interface which includes drawing functions, editing capabilities, and static and dynamic calculation features. The simulation functions offered by PowerFactory include power flow analysis, contingency analysis, optimal power flow among many other functions. In this report, we focus on power flow analysis capabilities and refer to [17] for further details. PowerFactory is licensed by DIgSILENT GmbH.

PowerFactory offers both AC and DC load power methods. In AC power flow method, the user can select one of the following formulations for solving the power flow problem.

1. Newton-Raphson power mismatch
2. Newton-Raphson current mismatch

PowerFactory allows the calculation of both balanced and unbalanced power flows. It is claimed in [17] that the Newton-Raphson power mismatch version converges best for large transmission systems, especially when heavily loaded and the Newton-Raphson current mismatch version converges best for unbalanced distribution systems. However, as we saw in section 4.1, the current-mismatch formulation can also be used for transmission systems.

In DC power flow method, only active power flow without losses is considered as explained in section 4.3 with the linear system (4.14).

PowerFactory has options for integration with Python scripts. Python scripts are generally used with PowerFactory for automation of tasks, creation of user defined calculation commands and integration of PowerFactory into other applications. PowerFactory also supports interfaces for softwares such as PSS®E and MATLAB.

5.2 PSS®E

PSS®E is a power system simulation and analysis tool for power transmission operation and planning. Similar to PowerFactory, it offers a wide range of simulation functions. For AC power flow calculations, PSS®E has the following iterative schemes along with a few other modified methods available.

1. Gauss-Seidel
2. Newton-Raphson
3. Decoupled Newton-Raphson

Since the convergence properties of solvers depend on the network and load attributes, the following procedure is suggested in [18] to solve the power flow problem, particularly in situations where the characteristics of new power flow problems are not known.

1. Use flat start values as initial values.
2. Execute Gauss-Seidel method until the corrections made to voltages and angles decrease to, for instance, 0.01 or 0.005 pu in consecutive iterations.
3. Switch to Newton-Raphson method and execute it until the problem converges or until there are signs of failure to converge.
4. If Newton-Raphson method does not converge within 8 to 10 iterations, switch back to Gauss-Seidel.

PSS®E also has an embedded Python interpreter which can be used to access and run models in PSS®E from Python scripts.

5.3 pandapower

pandapower is an open source tool for power system modelling, analysis and optimization with a high degree of automation. pandapower combines the data analysis library pandas and the power flow solver PYPOWER to create a network calculation program. PYPOWER is a port of MATPOWER to the Python programming language. MATPOWER offers the following power flow methods and a few other modified ones.

1. Newton-Raphson
2. Newton-Rapshon with Iwamoto multiplier
3. Gauss-Seidel
4. Fast decoupled load flow
5. DC power flow

MATPOWER includes four algorithms for solving the AC power flow problem which correspond to the four fundamental Newton-Raphson formulations: power and current mismatch formulations with polar and cartesian coordinates. The implementation of these formulations in MATPOWER is based on [9]. The default solver uses the power mismatch formulation with polar coordinates of the Newton-Raphson method (see section 4.1.1). It is mentioned in [19] that the Gauss-Seidel method is included only for academic interests as it has many disadvantages compared to the Newton's method.

By default, the AC power flow solvers in MATPOWER solve the power flow problem without considering voltage limits, line current limits and generator limits. Currently, none of the solvers include options for automatic updating of transformer taps and for satisfying constraints such as voltage limits [19]. However, there is an option to keep the generator reactive power within limits, but at the expense of voltage setpoints. That is, when the generator reactive power is kept within limits to ensure convergence, the voltages could go beyond the safe operating range which is generally set to 0.9 to 1.1 pu. This is based on a brute force technique which adds an outer loop around the AC power flow solver. If the reactive power limit of a generator is violated, the reactive power injection by that generator is force fixed at the limit and the power flow is solved again. This procedure is repeated until there are no more violations.

MATPOWER offers many benchmark grids to evaluate power flow algorithms. For our project, we consider the following test cases which represent parts of the European high voltage transmission network.

- Case 1354pegase: 1354 buses, 1751 lines.
- Case 2869pegase: 2869 buses, 4051 lines.
- Case 9241pegase: 9241 buses, 13797 lines.

Chapter 6

Conclusion

We draw the following conclusions from the literature review.

The power flow problem is the problem of finding the voltage magnitudes and phase angles in every bus of the network. The voltage phasors are then used to determine the line currents and thus the power flow in every line of the network. The power flow problem is a non-linear system of equations for which a closed-form solution does not exist. However, a numerical solution can be found by using iterative algorithms such as the Newton-Raphson method.

The Newton-Raphson method is widely regarded as the most distinguished full power flow solver. It is a root finding iterative algorithm that is used to solve a system of non-linear equations of the form $F(x) = 0$. Among several formulations of the NR method found in the literature, the current mismatch version with polar and Cartesian coordinates are found to perform the best for transmission networks [9]. The classical Newton-Raphson method has local quadratic convergence. Meaning, the method has quadratic convergence when the initial value is close to the solution. However, to achieve global convergence, that is to achieve convergence for any initial value, further modifications of the method are necessary. Furthermore, when the problem is ill-posed, the classical NR method tends to diverge.

The optimal multiplier method is commonly used to solve ill-posed power flow problems. That is, the optimal multiplier method helps to avoid false divergence and convergence to incorrect solutions, and also ensures global convergence. Using the optimal multiplier method, the existence of the solution from an initial value can be easily judged and if a solution exists, the power flow solution never diverges [14]. The optimal multiplier method is also known as Iwamoto multiplier method. To determine the optimal multiplier in every iteration of the NR method, the linesearch is an efficient technique that is commonly used [15].

The DC power flow method can be considered feasible to solve the power flow problem if the ratio of reactance to resistance X/R is greater than 4 [16].

We could find little material in the literature about automating power flow simulations. The closest we have found is a subroutine in MATPOWER that keeps generator reactive power within limits at the expense of voltage setpoints. This is not a mathematical approach but a brute force technique [19].

The software PowerFactory has a Python Application Programming Interface (API) that makes the functionality of PowerFactory accessible from a Python script. The API can be used to develop an interface in Python which can access the grid models and run simulations in PowerFactory. This functionality is currently used in the industry and academia to automate certain calculations in PowerFactory. However, the API is meant more to make the PowerFactory functionalities better accessible than to extract the grid models from PowerFactory and solve them on a different solver such as pandapower for the purpose of research.

Research Questions

In this project we focus on two main research questions: automating AC power flow simulations and comparison of AC and DC power flow methods. The two research objectives correspond to two applications respectively: reactive power compensation assessment and capacity planning.

1. **Automating AC power flow simulations**: The goal is to develop an automated solver which can perform AC year-round simulations for the European high voltage transmission network model, in order to perform reactive power compensation calculations. We take the following steps in order to develop the automated model.

   - The European transmission network model is found to be the one which has convergence issues the most. However, the exact reason for divergence is not clear yet. We investigate the European grid model in detail and find the possible reasons for the solver to diverge. We start with the fact that even though the European grid model converges for a particular set of inputs, it is found to diverge when the inputs change.
   - We use the Newton-Raphson formulations described in section 4.1 to develop the automated solver for the European grid model. This involves developing mathematical methods such as the optimal multiplier method that ensure convergence and also coming up with techniques to keep the voltages across the transmission network within limits, run-time, during year-round simulations.

- To achieve the above objectives, the bottleneck is that the European grid model is built in PowerFactory, the solvers of which cannot be accessed and modified. We try to use the Python API to develop an interface which can translate the grid models of PowerFactory to grid models that can be used in pandapower (see fig. 6.1).
- We start the implementation of algorithms in pandapower with test networks that are described in the next section.

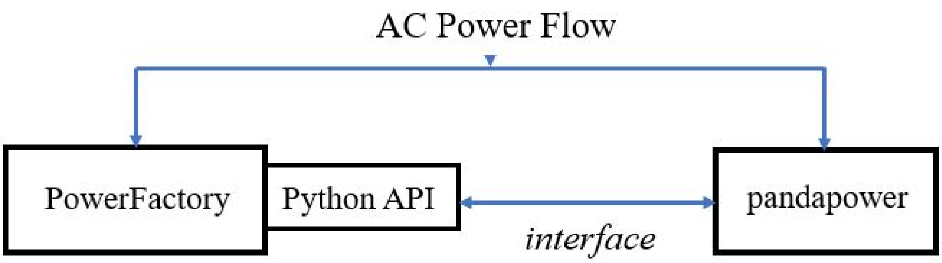

Figure 6.1: PowerFactory to pandapower

2. **AC vs DC approach**: The solutions of the AC power flow simulation models will be compared with the DC solutions. The consensus at the moment is that a difference in results higher than 5% makes AC power flow simulations justifiable for capacity planning. If the AC power flow method is found to be better than the DC approach, we make a cost analysis of the AC power flow method for doing year-round simulations. We start the comparison with the decisive factors that are described in section 4.5 (AC vs DC approach), which give a framework for the DC solutions to be considered feasible.

Transmission Networks

We consider the following transmission networks from TenneT for our experiments in this project.

1. 220 and 380 kV Dutch grid: 465 buses.
2. 110, 150, 220 and 380 kV Dutch grid: 1500 buses (see fig. 6.2).
3. The European grid which includes the 220, 380 kV Dutch grid connected to Germany, Belgium, Luxemburg and France: 12400 buses.

Figure 6.2: Grid map Netherlands

To test the algorithms, the test networks shown in table 6.1 that are available in pandapower will be considered.

Table 6.1: Test networks in pandapower

Test case	Buses	Lines	Loads	Shunts	Generators
1354pegase	1354	1751	621	1082	259
2869pegase	2869	4051	1311	2197	509
9241pegase	9241	13797	4461	7327	1444

Bibliography

[1] Carl Sulzberger. Pearl street in miniature: Models of the electric generating station [history]. *IEEE Power and Energy Magazine*, 11(2):76–85, 2013.

[2] TenneT. Electricity Producers: The Netherlands and Germany.

[3] Pieter Schavemaker and Lou van der Sluis. *Electrical Power System Essentials*. John Wiley & Sons, Inc., Sussex, United Kingdom, 2008.

[4] Alexandra von Meier. *Electric Power Systems*. John Wiley & Sons, Inc., Hoboken, NJ, USA, 2006.

[5] M.E. Kootte, J.E. Romate, and C. Vuik. Load Flow Computations for (Integrated) Transmission and Distribution Systems. A Literature Review. Technical report, Delft University of Technology, 2020.

[6] Fons van der Plas. *Power Grid Failures*. Thesis bsc mathematics, Radboud University Nijmegen, 2019.

[7] R. Idema, D.J.P. Lahaye, and C. Vuik. Load Flow Literature Survey. Technical report, Delft University of Technology, 2009.

[8] Brian Stott. Review of Load-Flow Calculation Methods. *Proceedings of the IEEE*, 62(7):916–929, 1974.

[9] Baljinnyam Sereeter, Cornelis Vuik, and Cees Witteveen. On a comparison of Newton–Raphson solvers for power flow problems. *Journal of Computational and Applied Mathematics*, 360:157–169, 2019.

[10] William. F. Tinney and Clifford E. Hart. Power Flow Solution by Newton's Method. *IEEE Transactions on Power Apparatus and Systems*, PAS-86(11):1449–1460, 1967.

[11] B. Stott and O. Alsac. Fast decoupled load flow. *IEEE Transactions on Power Apparatus and Systems*, PAS-93(3):859–869, 1974.

[12] Thomas J. Overbye, Xu Cheng, and Yan Sun. A comparison of the AC and DC power flow models for LMP calculations. In *Proceedings of the Hawaii International Conference on System Sciences*, volume 37, pages 725–734, 2004.

[13] James L. Kirtley. *Electric power principles: sources, conversion, distribution, and use*. John Wiley & Sons, Ltd, 2010.

[14] S. Iwamoto and Y. Tamura. A load flow calculation method for ill-conditioned power systems. *IEEE Transactions on Power Apparatus and Systems*, PAS-100(4):1736–1743, 1981.

[15] Patricia Rousseaux and Thierry Van Cutsem. Quasi steady-state simulation diagnosis using Newton method with optimal multiplier. In *2006 IEEE Power Engineering Society General Meeting, PES*. IEEE Computer Society, 2006.

[16] Konrad Purchala, Leonardo Meeus, Daniel Van Dommelen, and Ronnie Belmans. Usefulness of DC power flow for active power flow analysis. In *2005 IEEE Power Engineering Society General Meeting*, volume 1, pages 454–459, 2005.

[17] DIgSILENT GmbH. PowerFactory User Manual. Technical report, 2020.

[18] SIEMENS. PSSE Program Operation Manual. Technical report, 2017.

[19] MATPOWER. User's Manual, version 7.1. Technical report, 2020.